RI 8781

Bureau of Mines Report of Investigations/1983

Above-the-Earth Field Contours for a Dipole Buried in a Homogeneous Half-Space

By Steven M. Shope

UNITED STATES DEPARTMENT OF THE INTERIOR

Report of Investigations 8781

Above-the-Earth Field Contours for a Dipole Buried in a Homogeneous Half-Space

By Steven M. Shope

UNITED STATES DEPARTMENT OF THE INTERIOR
James G. Watt, Secretary

BUREAU OF MINES
Robert C. Horton, Director

This publication has been cataloged as follows:

Shope, Steven M

Above-the-earth field contours for a dipole buried in a homogeneous half-space.

(Bureau of Mines report of investigations ; 8781)

Includes bibliographical references.

Supt. of Docs. no.: I 28.23:8781.

1. Mine rescue work–Equipment and supplies. 2. Mine communication systems. 3. Electromagnetic fields. 4. Magnetic dipoles. I. Title. II. Series: Report of investigations (United States. Bureau of Mines) ; 8781.

TN23.U43 [TN297] 622s [622'.8] 82-600362

CONTENTS

ILLUSTRATIONS

TABLE

ABOVE-THE-EARTH FIELD CONTOURS FOR A DIPOLE BURIED IN A HOMOGENEOUS HALF-SPACE

By Steven M. Shope [1]

ABSTRACT

An essential element of the Bureau of Mines electromagnetic location and communication system for trapped miners is a quantitative knowledge of the surface and above-surface electromagnetic fields created by an underground transmitter. The field solutions given in this report use approximations in which the displacement currents are negligible for low frequencies. The earth is represented by a homogeneous half-space model in which a dipole source is immersed. The vertical magnetic field equipotential contours at and above the surface are graphically mapped. The volumes of the regions bounded by these contours are directly related to the geometrical zones of signal detectability. Knowledge of the detectability zones will enable the proper search strategies to be developed for airborne detection of trapped miners.

[1]Electrical engineer, Pittsburgh Research Center, Bureau of Mines, Pittsburgh, Pa.

INTRODUCTION

In response to the 1969 Coal Mine Health and Safety Act, the Bureau of Mines has maintained a research effort aimed at increasing the survivability of miners trapped underground following a disaster. A principal element of this effort is to develop a practical and effective means to detect, locate, and communicate with miners who cannot evacuate the mine immediately following a disaster. In 1970, the National Academy of Engineering[2] reported that an electromagnetic (EM) communications technique may be used for this purpose. Since the 1970 report was issued, the Bureau has sponsored a continued effort toward developing an EM communication and location system for postdisaster use. These programs have reached the stage where practical voice frequency (VF) signaling hardware has been developed for use by trapped miners.[3]

The Bureau is now in the process of developing suitable guidelines for the eventual implementation of such a system in the mining community. Included in such guidelines will be search strategies to be utilized by surface rescue teams to detect, locate, and rescue trapped miners. At mines where large surface areas need to be searched, airborne equipment will be employed to determine the general locale of the trapped miner's position. Surface personnel will then provide a more accurate location of the signal source. Therefore, a necessary component in formulating search strategies is a quantitative knowledge of the surface and above-the-surface EM field characteristics produced by the trapped miner's loop antenna.

Previous research has shown the relationship between probability of detection and signal strength, noise, receiver operating characteristics, depth, magnetic moment, and other factors.[4] It is assumed that search strategies will be developed that will enable rescue teams to define a satisfactory probability of detection for a particular disaster. Knowledge of noise statistics along with equipment and operator characteristics will determine the minimum signal strength required to achieve this particular detection probability.

The "zone of detectability" is defined as the geometrical volume in which the surface and above-surface field strengths of an EM signal are greater than or equal to the minimum value required for the desired probability of detection. Knowledge of this zone would enable rescue teams to search the surface in an effective and efficient manner.

This report analyzes the surface and above-the-earth fields (in particular H_z, the vertical magnetic field) and notes the effect of the electrical properties of the mine overburden on the field distributions. The fields are presented as two-dimensional cross-sectional views of the field strength contours mapped on a normalized Z-D (Z, vertical; D, horizontal) graph. Z and D are the vertical and horizontal dimensions normalized to the depth of the mine. The volume generated by rotating these contours 360° about the Z axis at D = 0 is also provided. This is valid because of the rotational symmetry of the vertical magnetic field.

[2]National Academy of Engineering. Mine Rescue and Survival (contract S0190606). BuMines OFR 4-70, 1970, 81 pp.; NTIS PB 191 691.

[3]General Instrument Corp. Development and Prototype Production of a Trapped Miner Signaling Transmitter/Transceiver (contract J0395017). Final Rept., 1980, 80 pp. Available for consultation at Pittsburgh Research Center, Bureau of Mines, Pittsburgh, Pa.

[4]Arthur D. Little, Inc. Detection of Trapped Miner Signals Above Coal Mines (contract J0188037). Final Rept., 1980, 288 pp. Available for consultation at Pittsburgh Research Center, Bureau of Mines, Pittsburgh, Pa.

FIELD SOLUTIONS

The electromagnetic field structure for an oscillating magnetic antenna has been thoroughly investigated by Wait and Campbell.[5] Their derivations include line sources, dipoles, finite-sized loops, and other kinds of signal sources, and have also considered the effects of layering in the earth half-space.

In particular, Wait and Campbell have presented the surface fields due to a magnetic dipole buried in a homogeneous half-space. Their solution is similar to that developed in the appendix of this report; the only difference results from the use of a different coordinate origin in the model. Without claim to originality, the Bureau of Mines derivation has been included to supplement the technical discussion in the main text of this report. Throughout this report, the rationalized MKSA (meter, kilogram, second, ampere) unit system is employed.

As derived in the appendix, the solution for the normalized magnetic field, defined as Q, on or above the surface is expressed by

$$Q = \int_0^\infty \frac{h^3 J_0(\lambda\rho)\lambda^3 e^{\lambda(h-z)-k_1 h}}{(\lambda+k_1)}\, d\lambda \ .$$

NUMERICAL EVALUATION

The above expression for Q is evaluated by numerical integration, specifically, 12-point Gaussian quadrature. Before this is done, however, the integrand is simplified if the dimensional variables are normalized with respect to the depth of loop burial, h. The following dimensionless, transformed variables are introduced:

$$D = \rho/h, \quad Z = z/h, \quad \text{and} \quad H = (\mu\omega\sigma)^{1/2}h.$$

H is not subscripted, but it is assumed to apply to the electrical properties of the earth half-space; H above the earth is zero. The factor H may be associated with the depth of loop burial divided by skin depth. The wave number k in region 1 (fig. A-1, appendix) becomes

$$k = \frac{1}{h}\,(x^2+iH^2)^{1/2},$$

where x is a new variable of integration:

$$x = \lambda h.$$

The expression for Q now appears as

$$Q = \int_0^\infty \frac{x^3 e^{-(x^2+iH^2)^{1/2}+x(1-Z)}}{x+(x^2+iH^2)^{1/2}} J_0(xD)dx \ .$$

Q has been evaluated at D = 0 and Z = 1 (coaxial at the surface) and is shown graphically in figure 1 as a function of H. The rapid decrease in Q as H increases is readily seen in this figure. Physically, this may be interpreted as the effect the electrical properties of the half-space have upon the surface field strength. For a fixed burial depth, H is inversely related to the skin depth; thus, Q falls off proportionally to skin depth as seen in figure 1.

CONTOURING

Q is a multivalued function that is not readily adaptable to conventional contouring methods. The contours presented here were generated by first creating a data grid of $Q(D_i, Z_j)$ values for D = 0 to 10 and Z = 1 to 10. Each grid element was obtained by numerically evaluating the integral expression for Q. The increment of the D coordinate was 0.010, and that of the Z coordinate was

[5] Wait, J. R., and L. L. Campbell. The Fields of an Oscillating Magnetic Immersed in a Semi-Infinite Conducting Medium. J. Geophys. Res., v. 58, No. 2, June 1953.

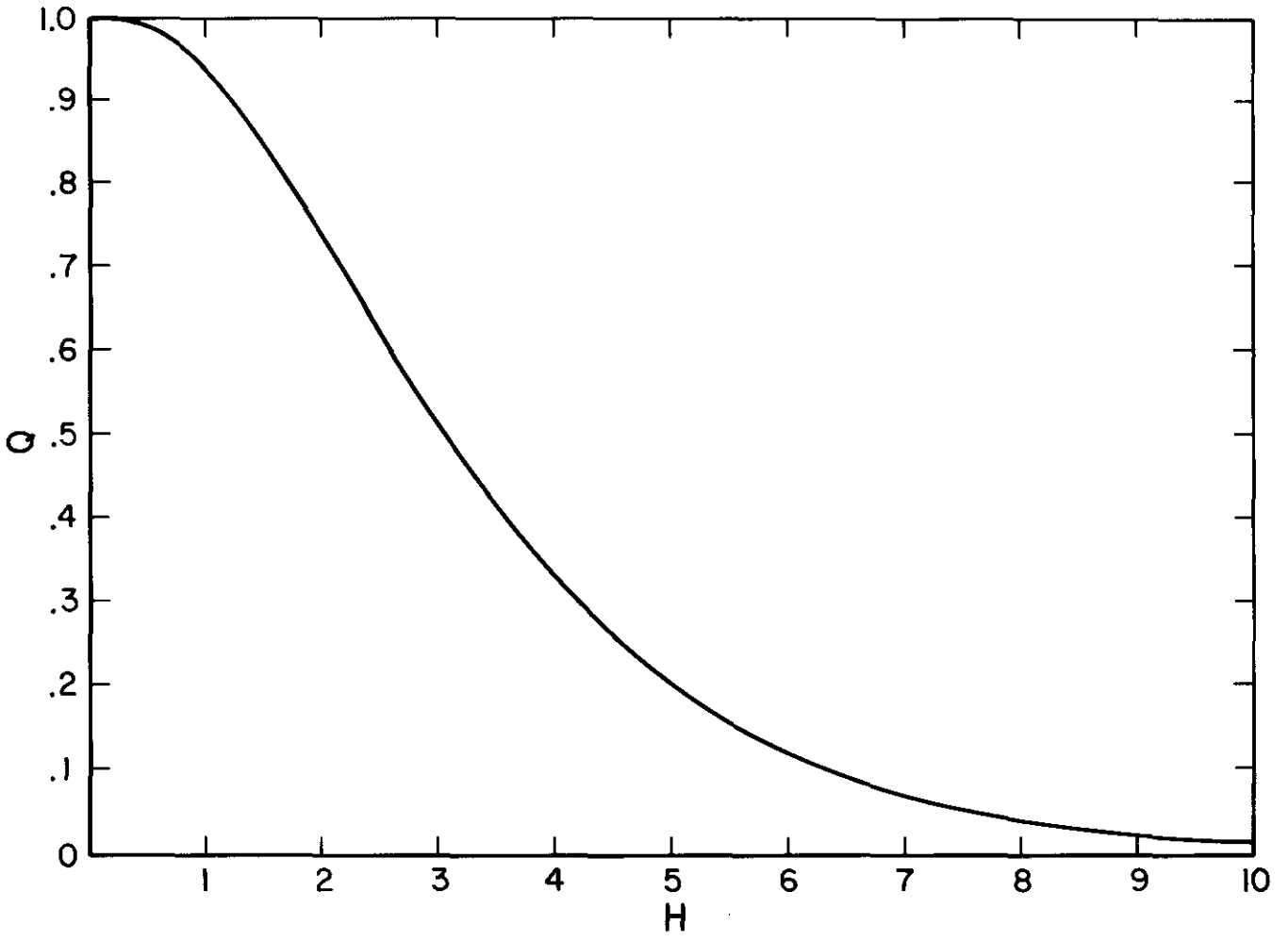

FIGURE 1. - Normalized vertical magnetic field (Q) versus H.

0.080. This resulted in a data grid containing over 125,000 elements for each value of H. For a particular Q value to be contoured, denoted Q_c, the data grid values $Q(D_i, Z_j)$ were searched for an inflection about Q_c. This procedure alleviated problems associated with the fact that Q is multivalued. For this report, the following Q_c values were contoured:

Q = 0.001, 0.005, 0.010, 0.050, 0.100, for 10 values of H:

H = 0.0, 0.10, 0.50, 0.80, 1.0, 2.0, 4.0, 6.0, 8.0, 10.0.

The contours were then mirrored into the (-D,+Z) quadrant since the surface and above-surface fields must be symmetrical about the Z axis. In figure 2, the Q contours are graphically presented. Because of the size of the increment in the data grid, the resolution of the contours may be slightly limited in some of the figures; however, the general shape is very apparent. Note that the graphs in figures 2*F* through 2*J* have a larger scale vertical axis.

In this set of contour figures, the Q contours are composed of primary and secondary lobes. For the free-space condition, H = 0, the lobes are very distinct. However, as Q_c increases, the secondary lobes disappear. Also, as H increases, the primary and secondary lobes become distorted and less distinct, and the lobe size diminishes. This last result is physically intuitive since the attenuative effects of the earth would limit

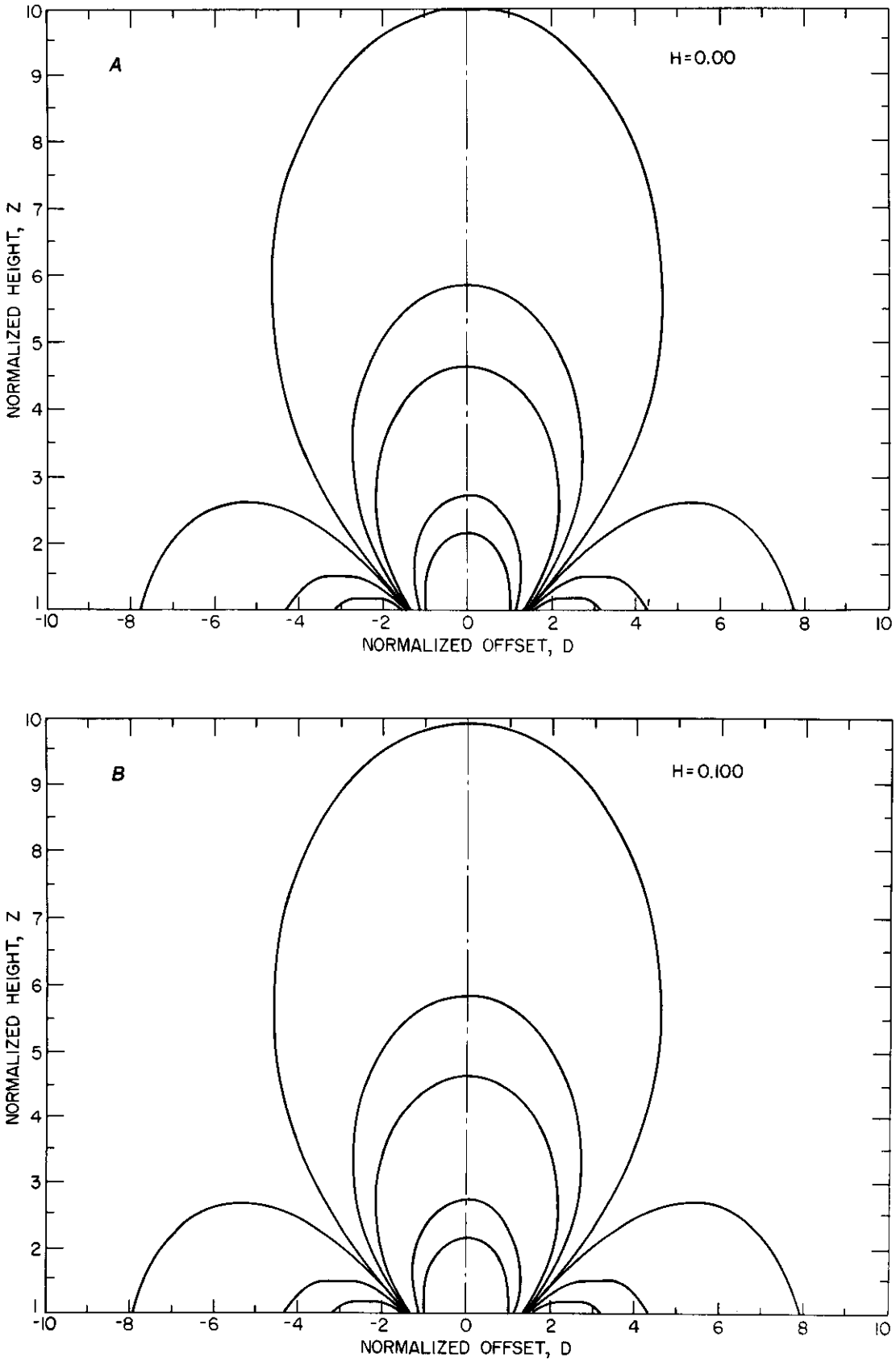

FIGURE 2. - Normalized vertical magnetic field contours. *A*, H = 0.00; *B*, H = 0.100.

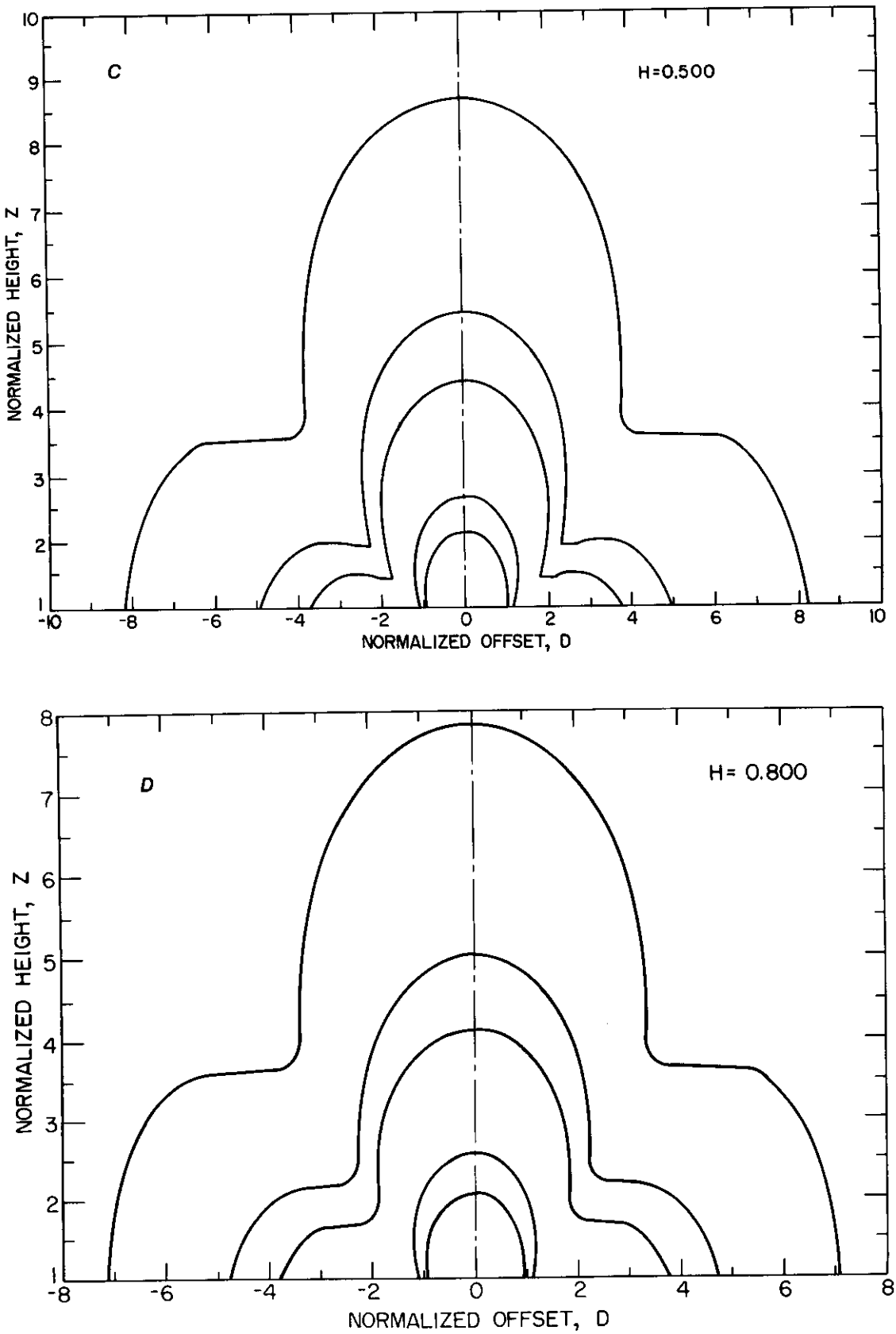

FIGURE 2. - Normalized vertical magnetic field contours–Continued. *C*, H = 0.500; *D*, H = 0.800.

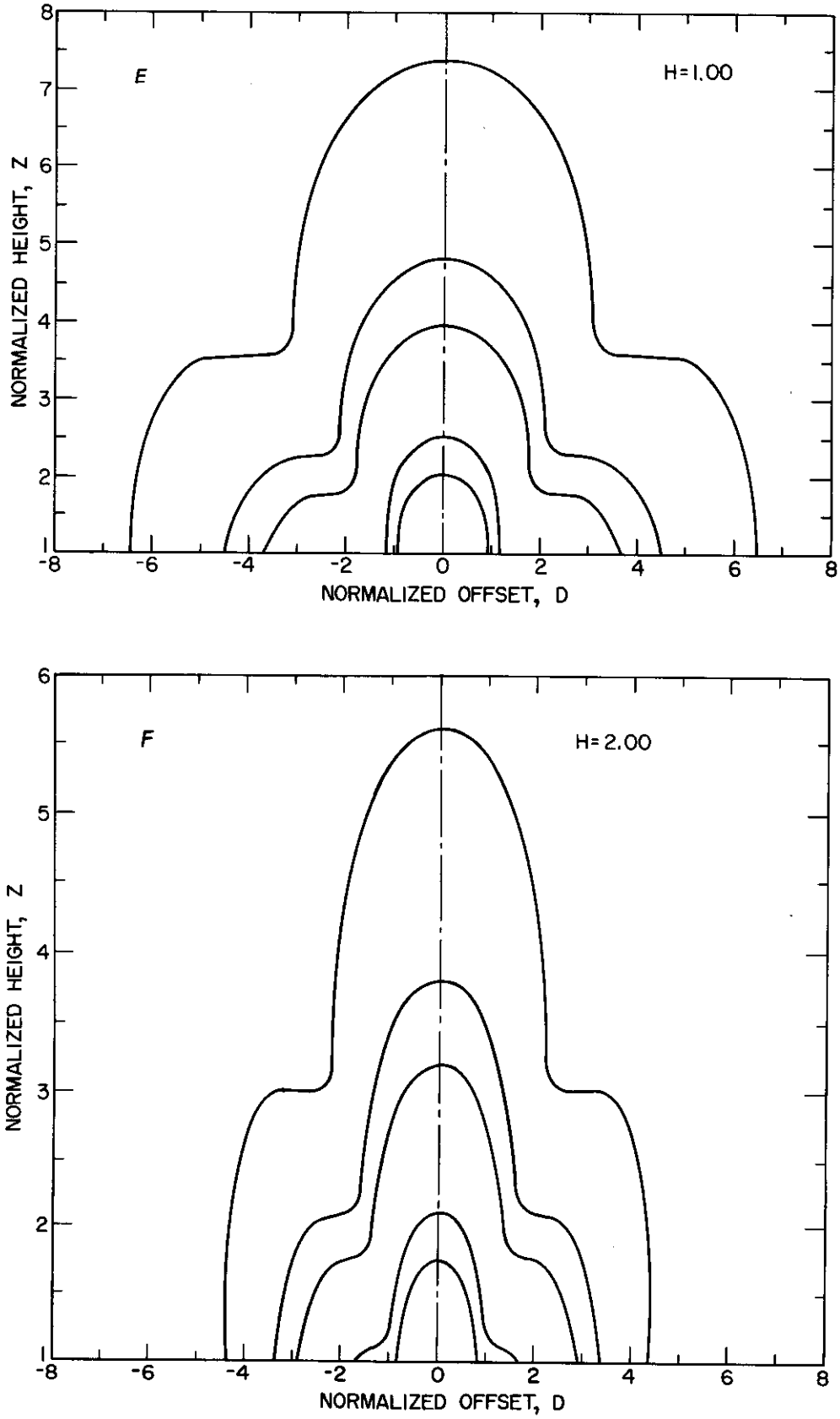

FIGURE 2. - Normalized vertical magnetic field contours–Continued. *E*, H = 1.00; *F*, H = 2.00.

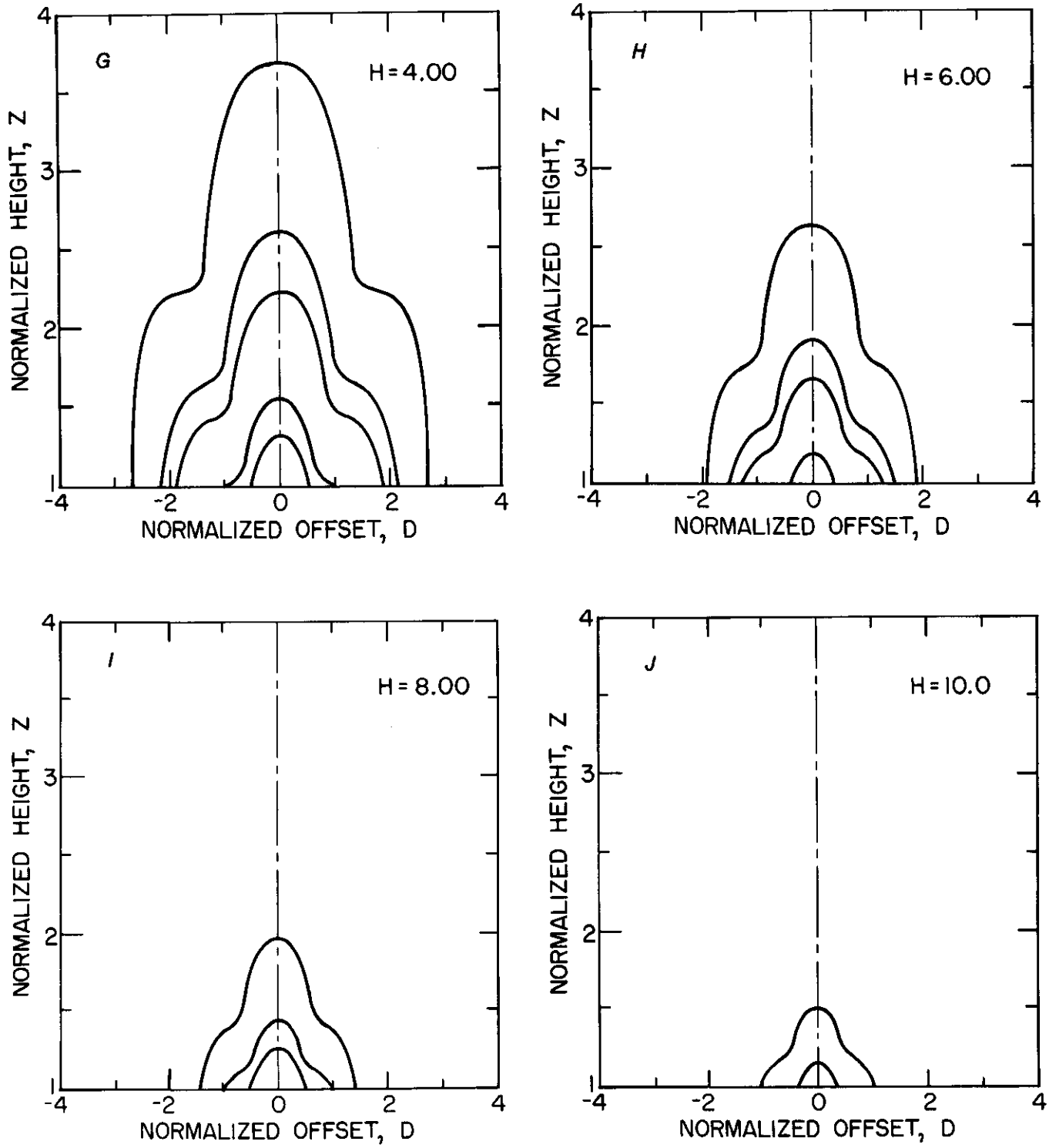

FIGURE 2. - Normalized vertical magnetic field contours–Continued. *G*, H = 4.00; *H*, H = 6.00; *I*, H = 8.00; *J*, H = 10.0.

the field pattern. To obtain a general idea of the decrease in size, the approximate volumes of each contour were calculated by rotating them about the Z axis. Volume, as used here, is dimensionless (since Z and D are also dimensionless) and may be thought of as a normalized volume. Since the normalization is to depth cubed, actual volume values could be readily calculated for any particular mine depth. The volumes are listed in table 1 and plotted on a semilog plot versus H in figure 3.

This graph shows that the lobe volume for a particular Q contour may be fitted to the expression

$$Vol_c = \text{constant} \cdot 10^{c \cdot H},$$

where c is a constant and has been found empirically to be approximately -1/3.

TABLE 1. - Normalized lobe volumes of all contours graphed

Q contour.....	0.001	0.005	0.010	0.050	0.100
H = 0.00:					
Primary.....	401.900	78.860	38.520	6.500	2.67
Secondary.....	210.200	17.840	2.950	.000	.00
Total.....	612.200	96.700	41.470	6.500	2.67
H = 0.100:					
Primary.....	409.200	78.120	38.290	6.490	2.67
Secondary.....	198.200	18.290	3.030	.000	.00
Total.....	607.900	96.410	41.320	6.490	2.67
H = 0.500:					
Primary.....	636.700	106.600	42.800	5.870	2.47
Secondary.....	.000	1.580	.983	.000	.00
Total.....	636.700	108.900	43.830	5.870	2.47
H = 0.800:					
Primary.....	470.600	101.900	45.400	5.060	2.18
Secondary.....	.000	.000	.000	.000	.00
Total.....	470.600	101.900	45.400	5.060	2.18
H = 1.00:					
Primary.....	376.700	90.730	42.470	4.530	1.95
Secondary.....	.000	.000	.000	.000	.00
Total.....	376.700	90.730	42.470	4.530	1.95
H = 2.00:					
Primary.....	139.600	41.400	22.100	2.890	1.000
Secondary.....	.000	.000	.000	.000	.000
Total.....	139.600	41.400	22.100	2.890	1.000
H = 4.00:					
Primary.....	30.830	9.600	5.140	.555	.158
Secondary.....	.000	.000	.000	.000	.000
Total.....	30.830	9.600	5.140	.555	.158
H = 6.00:					
Primary.....	8.670	2.380	1.090	.050	.000
Secondary.....	.000	.000	.000	.000	.000
Total.....	8.670	2.380	1.090	.050	.000
H = 8.00:					
Primary.....	2.540	.442	.109	.000	.000
Secondary.....	.000	.000	.000	.000	.000
Total.....	2.540	.442	.109	.010	.000
H = 10.0:					
Primary.....	.624	.028	.000	.000	.000
Secondary.....	.000	.000	.000	.000	.000
Total.....	.624	.028	.000	.000	.000

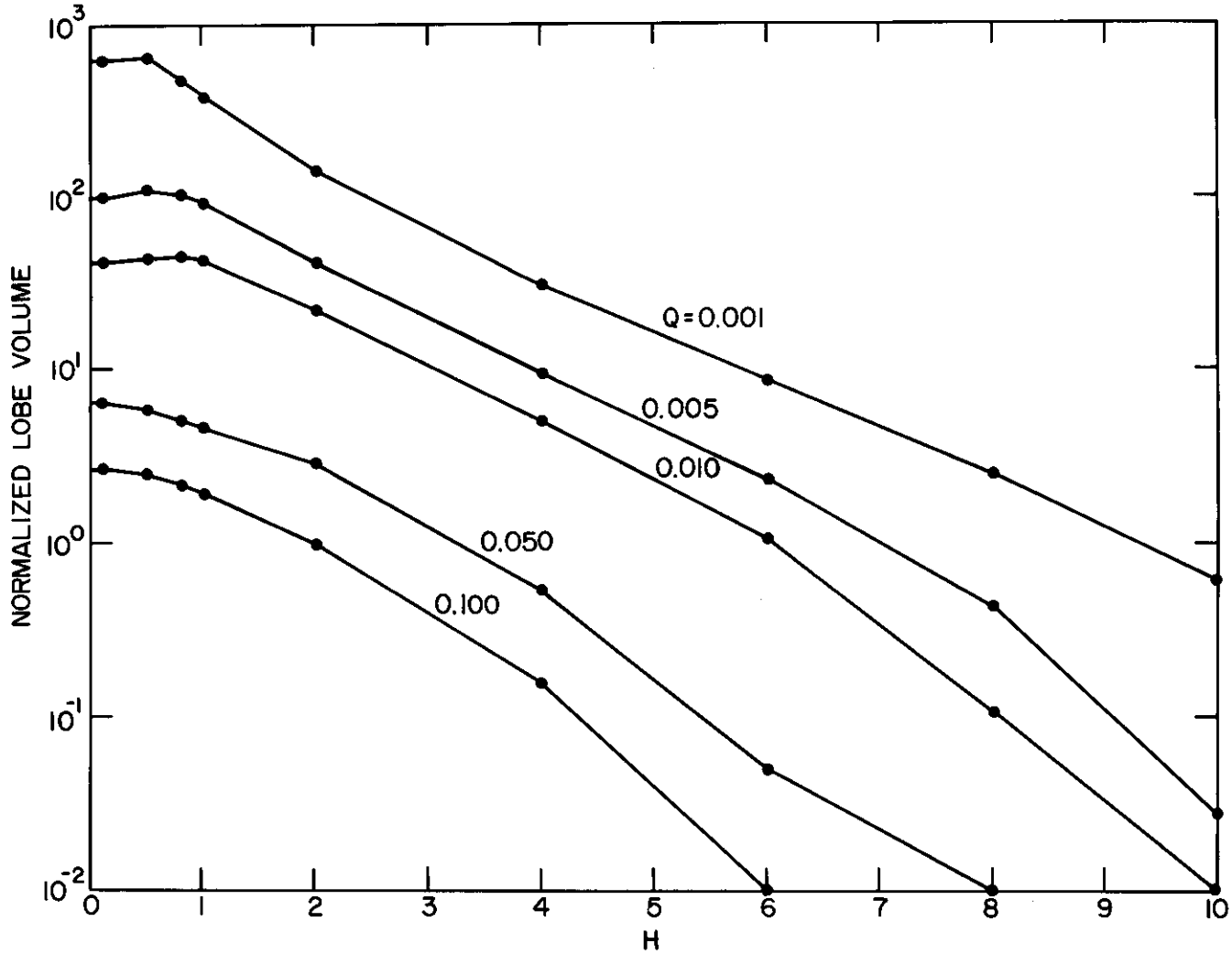

FIGURE 3. - Normalized volume of vertical magnetic field contour versus H.

CONCLUSIONS

Several normalized vertical magnetic field (Q) contours for various overburden characteristics (H) have been presented graphically. The general shape of the contours remains consistent for all values of Q contoured; however, the vertical and horizontal ranges rapidly diminish with increasing Q, as would be expectd. The multilobe characteristic of the smaller value Q contours vanishes for Q larger than about 0.010.

The overburden characteristics, as expressed by H, along with mine depth (h), have been previously measured at a variety of mines across the United States. This data base has enabled a statistical description of the distribution of H and h for all U.S. coal mines.[6] Utilizing this, along with receiver detectability data, efficient airborne search strategies can be developed for detecting a trapped miner's signal as rapidly as possible. As an example, one may visualize from the contour plots that the radial range on the surface of the multilobe contours (e.g., Q = 0.001) is up to 16 times the mine's depth. However, since there are primary and secondary lobes, one must be careful not simply to use a

[6]Work cited in footnote 4.

signal maximum as an indication of the trapped miner's coaxial axis (D = 0). If a probability of detection has been defined requiring a surface or above-the-surface field strength, H_z min, then the minimum detectable Q can be expressed as

$$Q = \left| \frac{H_z \text{ min}}{-b} \right| ,$$

where b is the free-space vertical magnetic field strength. This assumes prior knowledge of the magnetic moment underground, the mine depth, and overburden conductivity. This minimum detectable Q will define the physical region of signal detectability, which may be determined from the contours developed in this report.

NOMENCLATURE

A ratio of loop radius to mine depth

a radius of circular current loop

b free-space vertical magnetic field strength

D horizontal surface offset divided by mine depth

d horizontal surface offset

E electric field strength

H ratio of skin depth to mine depth

H_z vertical magnetic field strength

h depth of loop burial (mine depth)

I current in loop

J_m mth order Bessel function

k wave number

M magnetic moment

Q normalized vertical magnetic field

Y_m mth order of Neumann function

Z vertical height above surface divided by mine depth

z vertical height above surface

ε dielectric permittivity

μ magnetic permeability

Π^* magnetic vector potential

σ ohmic conductivity

ψ amplitude coefficient

ω angular frequency

APPENDIX.--FIELD SOLUTION DERIVATION

The regions below the earth's surface are treated as a homogeneous half-space processing an ohmic conductivity as expressed by σ and dielectric permittivity ϵ. The magnetic permeability μ of all regions in the problem is assumed to be that of free space, $\mu = \mu_o$.

The trapped miner's antenna is considered a circular current loop of radius a, oscillating at an angular frequency ω. The model is shown in figure A-1. The loop is located at a depth h below the surface and possesses a magnetic moment, M, entirely in the $\hat{z}$ direction. The geometry of the situation lends itself to the use of a circular cylindrical coordinate system with an origin at the loop axis. The loop axis divides the half-space into regions 1 and 2; the two regions are electrically identical, and the purpose of this additional boundary is to introduce the source term into the boundary conditions.

The solution of this problem is enhanced by using magnetic vector potentials, $\bar{\Pi}^*$, which are related to the electric and magnetic fields by the following expression derived from Maxwell equations:

$$\bar{E} = \mu \frac{\partial}{\partial t} (\bar{\nabla} \times \bar{\Pi}^*),$$

$$\bar{H} = - \bar{\nabla} (\bar{\nabla} \cdot \bar{\Pi}^*) + \mu\sigma \frac{\partial \bar{\Pi}^*}{\partial t} + \mu\epsilon \frac{\partial^2 \bar{\Pi}^*}{\partial t^2} .$$

It follows that Π^* must be a solution of the Helmholtz equation:

$$\nabla^2 \bar{\Pi}^* - \mu\epsilon \frac{\partial^2 \bar{\Pi}^*}{\partial t^2} - \mu\sigma \frac{\partial \bar{\Pi}^*}{\partial t} = 0.$$

Assuming Π^* has a $e^{-i\omega t}$ time dependence and making the substitution

$$- \gamma^2 = \mu\omega(\omega\epsilon + i\sigma),$$

the above differential equation becomes

$$\nabla^2 \bar{\Pi}_i^* - \gamma_i^2 \bar{\Pi}_i^* = 0,$$

where the subscript, i, denotes the geometrical region of the model. The vector potential $\bar{\Pi}^*$ is a vector quantity processing only a $\hat{z}$ component. Solutions to the above are of the form

$$\Pi_i^* = [J_m(\lambda\rho) + Y_m(\lambda\rho)][\cos m\phi + \sin m\phi][e^{k_i z} + e^{-k_i z}].$$

The $J_m(\lambda\rho)$ and $Y_m(\lambda\rho)$ terms are Bessel functions of the first and second kind, order m, respectively. The separation constant m is not restricted to integer values. The angular homogeneity allows no angular field variations, thus, m = o. Also, the solution must remain finite as $\rho \to o$, requiring the $Y_m(\lambda\rho)$ term to be excluded. The above solution requires the following separation constant relationship:

$$k_i^2 = \lambda^2 + \gamma_i^2.$$

The solution takes on the form

$$\Pi_i^* = J_o(\lambda\rho)\, e^{\pm k_i z},$$

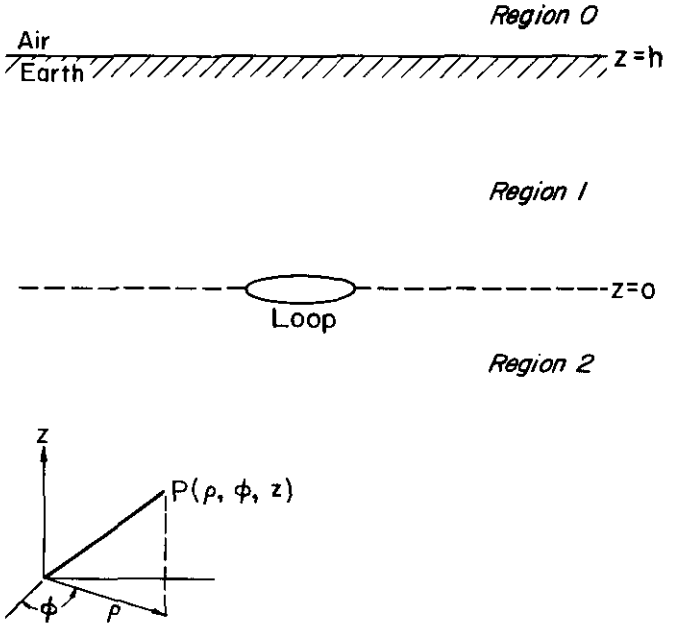

FIGURE A-1. - Dipole buried in a homogeneous half-space.

where k_i is the complex wave number. Since the plane wave propagation associated with $e^{k_i z}$ and $e^{-k_i z}$ need not be of equal amplitudes, the introduction of $\Psi_i^+(\lambda)$ and $\Psi_i^-(\lambda)$ generalizes the solution:

$$\Pi_i^* = J_0(\lambda\rho)\{\Psi_i^-(\lambda)e^{-k_i z} + \Psi_i^+(\lambda)e^{+k_i z}\},$$

and the complete solution is the superposition of all solutions:

$$\Pi_i^* = \int_0^\infty J_0(\lambda\rho)\{\Psi_i^-(\lambda)e^{-k_i z} + \Psi_i^+(\lambda)e^{+k_i z}\}d\lambda.$$

Since $\bar{\Pi}^*$ has only a $\hat{z}$ component, the electric field has only a $\hat{\phi}$ component and is of the form;

$$E_i = i\mu\omega\frac{\partial\Pi_i^*}{\partial\rho},$$

and the magnetic field has only $\hat{\rho}$ and $\hat{z}$ components:

$$\bar{H}_i = \frac{\partial^2\Pi_i^*}{\partial\rho\partial z}\hat{\rho} + (\gamma_i^2 - \frac{\partial^2}{\partial z^2})\Pi_i^*\hat{z}$$

In order to obtain explicit expressions for the components of $\bar{E}$ and $\bar{H}$, an explicit form for Π_i^* must first be obtained, which requires determination of the coefficients $\Psi_i^+(\lambda)$ and $\Psi_i^-(\lambda)$ for each region i. This is accomplished by applying the boundary conditions requiring continuity of tangential E and H at all boundaries except that at the source. The tangential E and H fields are

$$E_{\phi_i} = -i\mu\omega\int_0^\infty \lambda J_1(\lambda\rho)\{\Psi_i^-(\lambda)\, e^{-k_i z} + \Psi_i^+(\lambda)e^{+k_i z}\}d\lambda;$$

$$H_{\rho_i} = \int_0^\infty k_i\lambda J_1(\lambda\rho)\{\Psi_i^-(\lambda)e^{-k_i z} - \Psi_i^+(\lambda)e^{+k_i z}\}d\lambda.$$

The set of boundary conditions requires

(1) $H_{\rho_0} - H_{\rho_1} = o$ at $z = h$;

(2) $E_{\phi_0} - E_{\phi_1} = o$ at $z = h$;

(3) $H_{\rho_1} - H_{\rho_2} = j_\phi(\rho)$ at $z = o$;

(4) $E_{\phi_1} - E_{\phi_2} = o$ at $z = o$.

It can be seen in the third equation that H_ρ is discontinuous across the source boundary by an amount equal to the surface current density $j_\phi(\rho)$ (Ampere's law). Since the current loop antenna has been modeled as an infinitesimally thin ring of current, of radius a, $j_\phi(\rho)$ will be the source term for the field. Also, by inspection, the coefficients $\Psi_2^-(\lambda)$ and $\Psi_0^+(\lambda)$ are equated to zero since there are no sources below z = o or above z = h.

The source term $j_\phi(\rho)$ may be mathematically expressed as a two-dimensional current ring, using the Dirac delta function:

$$j_\phi(\rho) = I\delta(\rho-a)$$

where I is the current. This may be represented by a Fourier-Bessel integral:

$$j_\phi(\rho) = \int_0^\infty f(\lambda)J_n(\lambda\rho)\lambda d\lambda,$$

where the expansion coefficient $f(\lambda)$ is defined as

$$f(\lambda) = \int_0^\infty j_\phi(\rho)J_n(\lambda\rho)\rho d\rho$$

or $$f(\lambda) = \int_0^\infty I\delta(\rho-a)J_n(\lambda\rho)\rho d\rho\ .$$

After integrating,

$$f(\lambda) = IaJ_n(\lambda a).$$

Thus, the source term becomes

$$j_\phi(\rho) = \int_0^\infty IaJ_1(\lambda a)J_1(\lambda\rho)\lambda d\lambda,$$

where n = 1 has been chosen to keep the Fourier-Bessel representation of the current density in the same functional space as that of the H_ρ representation.

Although the details are not included, the four boundary value equations have

been solved simultaneously to yield an explicit expression for $\Psi_0^-(\lambda)$:

$$\Psi_0^-(\lambda) = \frac{IaJ_1(\lambda a)k_1 e^{(\lambda-k_1)h}}{\lambda+k_1} ,$$

using the dipole approximation that, for small λa,

$$2\frac{J_1(\lambda a)}{\lambda a} \rightarrow 1 .$$

However, the finite size of the loop may have an influencing effect on the surface and above-surface field structures in the limiting case of shallow loop burial and large loop dimensions. By disallowing the above approximation, the solutions may be adapted to account for the loop size. However, the dipole approximation is greater than 98 pct accurate for $A \leq 0.10$, where A is defined as the ratio of loop radius to mine depth. Hill and Wait have presented a detailed discussion of the finite-sized loop problem.[1] The rest of this derivation will assume the loop to be a dipole.

Then, $\Psi_0^-(\lambda)$ becomes

$$\Psi_0^-(\lambda) = \frac{Ia^2\lambda e^{(\lambda-k_1)h}}{2(\lambda+k_1)} .$$

As shown previously, the vertical magnetic field is defined as

$$H_{z_i} = \gamma_i^2 - \frac{\partial^2}{\partial z^2}\Pi_i^* .$$

For the region above the surface, $\gamma_0^2 = 0$; thus,

$$H_{z_0} = -\frac{\partial^2}{\partial z^2}\Pi_i^*$$

$$\text{or } H_{z_0} = -\int_0^\infty \frac{J_0(\lambda\rho)Ia^2\lambda^3 e^{(\lambda-k_1)h-\lambda z}}{2(\lambda+k_1)}\,d\lambda$$

In the main text of this report, the surface and above-the-surface vertical magnetic field are referred to as H_z with no region zero subscript.

The results presented are normalized to the field strength in free space for a coaxial source located at a distance h. The normalized factor is contained in b and explicitly defined as

$$b = \frac{INA}{2\pi h^3} ,$$

where INA = M, the magnetic moment; I is the current in the loop of area A and of N turns. H_z may be defined as

$$H_z = -bQ .$$

Thus, the loss mechanisms of the half-space and field strength diminishing due to observations above z = h are contained in Q. If the half-space were free space, then Q = 1 at z = h. Q is explicitly expressed as

$$Q = \int_0^\infty \frac{h^3 J_0(\lambda\rho)\lambda^3 e^{\lambda(h-z)-k_1 h}\,d\lambda}{(\lambda+k_1)} .$$

[1]Hill, D. A., and J. R. Wait. Analytical Investigations of Electromagnetic Location Schemes Relevant to Mine Rescue (contract H0122061, Inst. Telecommunication Sci.). BuMines OFR 25-75, 1974, 147 pp.

☆U.S. GOVERNMENT PRINTING OFFICE: 1983-605-015/52

INT.-BU.OF MINES,PGH.,PA. 26914